Journal of Pharmaceutical Analysis 7 (2017) 103–109

Contents lists available at ScienceDirect

Journal of Pharmaceutical Analysis

journal homepage: www.elsevier.com/locate/jpa

Original Research Article

Investigation of binding behaviour of procainamide hydrochloride with human serum albumin using synchronous, 3D fluorescence and circular dichroism

Kirthi Byadagi, Manjunath Meti, Sharanappa Nandibewoor, Shivamurti Chimatadar*

P.G. Department of Studies in Chemistry, Karnatak University, Dharwad 580003, India

ARTICLE INFO

Keywords:
Procainamide hydrochloride
Human serum albumin
Circular dichroism
Synchronous fluorescence
3D fluorescence

ABSTRACT

Interaction of procainamide hydrochloride (PAH) with human serum albumin (HSA) is of great significance in understanding the pharmacokinetic and pharmacodynamic mechanisms of the drug. Multi-spectroscopic techniques were used to investigate the binding mode of PAH to HSA and results revealed the presence of static type of quenching mechanism. The number of binding sites, binding constants and thermodynamic parameters were calculated. The results showed a spontaneous binding of PAH to HSA and hydrophobic interactions played a major role. In addition, the distance between PAH and the Trp–214 was estimated employing the Förster's theory. Site marker competitive experiments indicated that the binding of PAH to HSA primarily took place in subdomain IIA (Sudlow's site I). The influence of interference of some common metal ions on the binding of PAH to HSA was studied. Synchronous fluorescence spectra (SFS), 3D fluorescence spectra and circular dichroism (CD) results indicated the conformational changes in the structure of HSA.

1. Introduction

Serum albumin (SA) is a major protein in the circulatory system, which has been extensively studied among all proteins. It plays a significant role in many physiological functions [1] and serves as a model protein for studying drug–protein interaction in vitro [2]. Many drugs and other bioactive small molecules bind reversibly to SA [3,4], which implicates its role as a carrier. Therefore, the interaction of drugs and SA is significant for knowing the transport and distribution of drugs in the body, influence on drug toxicity and stability during the chemotherapeutic process [5].

Human serum albumin (HSA) is a principal extracellular protein with a high concentration in blood plasma [6,7]. The main role of HSA is to maintain the colloid osmotic pressure in the blood [8,9]. It is a globular protein composed of 585 amino acid residue monomer and three structurally similar domains (I, II and III), each containing two subdomains (A and B). HSA contains two principal drug binding sites, site I and site II, and only one tryptophan residue, Trp–214, in the subdomain IIA is capable of binding most drugs by strong hydrophobic interactions [10]. HSA is the most extensively studied protein because of its ready availability, biodegradability, immunogenicity and its lack of toxicity, making it an ideal candidate for drug delivery [11].

Procainamide hydrochloride (PAH) (Fig. S1), a pharmaceutical antiarrhythmic agent, is used for the medical treatment of cardiac arrhythmias. It is a sodium channel blocker which blocks open sodium channels and prolongs the cardiac action potential. This drug is used for both supraventricular and ventricular arrhythmias, as indicated in the treatment of premature ventricular contractions, ventricular tachycardia, atrial fibrillation, and paroxysmal atrial tachycardia [12]. The major active metabolite of PAH is N–acetylprocainamide (NAPA), which is approximately equipotent to the parent drug as an antiarrhythmic agent [13]. PAH measurement in plasma is advocated as a useful guidance to therapy.

The molecular interactions are often monitored by spectroscopic techniques [14] because these methods are sensitive and relatively easy to use. They have advantages over conventional approaches [15–17] which suffer from lack of sensitivity, use of excess concentration, and long analysis time for drug–protein interaction. In a series of studies, fluorescence techniques are great aids in the study of interactions between drugs and plasma proteins because of their high sensitivity, rapidity, and ease of implementation [18]. The pharmaceutical firms need standardized screens for protein binding in new drug design and fixing dose limits. Hence, in view of pharmaceutical importance of PAH, we studied the in vitro interaction of PAH with HSA using

Peer review under responsibility of Xi'an Jiaotong University.
* Corresponding author.
E-mail address: schimatadar@gmail.com (S. Chimatadar).

http://dx.doi.org/10.1016/j.jpha.2016.07.004
Received 26 July 2015; Received in revised form 15 July 2016; Accepted 17 July 2016
Available online 09 December 2016

fluorescence quenching method. In addition, displacement studies using site selective probes were performed and the conformational changes of HSA were discussed on the basis of synchronous fluorescence spectra (SFS), circular dichroism (CD) and 3D fluorescence results.

2. Experimental

2.1. Chemicals

HSA (Fraction V powder, fatty acid free) and PAH were obtained from Sigma Aldrich (St. Louis, MO, USA) and used without further purification. Warfarin, ibuprofen and digitoxin (analytical standard) were purchased from Sigma Aldrich (Bangalore, India). The stock solutions of HSA (66,000) and PAH (each 250 μM) were prepared in 0.1 M phosphate buffer of pH 7.4 containing NaCl. All chemicals were of analytical reagent grade and millipore water (ELIX–10 & MILLI–Q gradient, Bangalore, India) was used throughout the study.

2.2. Instruments

All fluorescence measurements were performed on a spectrofluorimeter Model F–7000 (Hitachi, Japan) equipped with a 150W Xenon lamp, a slit width of 5 nm and 1 cm quartz cell. The required temperature was maintained by circulating water bath (CYBERLAB CB 2000, MA, USA). The absorption spectra were recorded on a double beam CARY 50-BIO UV–vis spectrophotometer (Varian, Australia) equipped with a 150W Xenon lamp, a slit width of 5 nm and 1 cm quartz cell. The pH of solution was measured with an Elico LI120 pH meter (Elico Ltd., India). The CD measurements were made on a JASCO–715 spectropolarimeter (Tokyo, Japan) in a 0.2 cm quartz cell at room temperature.

2.3. Methods

2.3.1. Fluorescence quenching study

On the basis of preliminary investigations, intrinsic fluorescence of HSA was measured at 288, 298 and 308 K in the range of 250–500 nm upon excitation at 280 nm. The concentration of HSA was kept constant at 5 μM and that of the drug was varied from 5 to 45 μM.

2.3.2. UV–vis measurements

The UV–vis absorption measurements of HSA in the presence and absence of PAH were recorded in the range of 230–340 nm. The concentration of HSA was fixed at 5 μM while that of drug was varied from 0 to 45 μM. Then, the overlap of the UV absorption spectrum of PAH with the fluorescence emission spectrum of HSA was used to calculate the energy transfer. The absorbance values of drug-protein mixtures in the concentration range employed in the study did not exceed 0.05 at the excitation wavelength.

2.3.3. Displacement studies

The displacement experiments were performed using different site probes, i.e., warfarin, ibuprofen and digitoxin for sites I, II and III, respectively [19], by keeping the concentration of HSA and the probe constant (5 μM each) and varying the concentration of the drug. The fluorescence emission spectra were recorded and binding constant values of PAH–HSA–probe system were evaluated.

2.3.4. Effect of common ions

The effect of interference of some common ions like Zn^{2+}, Ca^{2+}, Cu^{2+}, Mn^{2+}, Ni^{2+} and Co^{2+} on PAH–HSA interactions was carried out. For this, the fluorescence spectra of PAH–HSA system were recorded in the presence of the above ions at 340 nm upon excitation at 280 nm. The overall concentration of HSA and that of the common ions were fixed at 5 μM.

2.3.5. CD

The CD measurements of HSA in the presence and absence of PAH were made in the range of 200–250 nm using a 0.2 cm path length cell at 0.2 nm intervals with three scans averaged for each spectrum. The HSA to drug concentration was varied (1:0, 1:1 and 1:3, v/v) and the CD spectrum was recorded.

2.3.6. Synchronous fluorescence

The synchronous fluorescence characteristics of PAH–HSA were measured at different scanning intervals of $\Delta\lambda$ ($\Delta\lambda=\lambda_{em}-\lambda_{ex}$). When $\Delta\lambda$=15 nm, the spectrum characteristic of protein tyrosine residues was observed, and when $\Delta\lambda$=60 nm, the spectrum characteristic of protein tryptophan residues was observed.

2.3.7. 3D fluorescence

For 3D fluorescence spectra, the emission wavelength was recorded between 200 and 600 nm and the initial excitation wavelength was set at 200 nm with an increment of 10 nm up to 350 nm. Other scanning parameters were identical to those of steady state fluorescence spectral studies.

3. Results and discussion

3.1. Fluorescence quenching of HSA induced by PAH in physiological conditions

For macromolecules, the fluorescence measurements can give some information such as the binding mechanism, binding mode, binding constants, binding sites, and intermolecular distance [20]. The fluorescence intensity of a compound can be decreased by a variety of molecular interactions [21]. The intrinsic fluorescence of HSA is almost contributed by tryptophan alone [22]. Fig. 1 shows the fluorescence emission spectra of HSA in the absence and presence of PAH. The addition of PAH led to a concentration dependent quenching of HSA intrinsic fluorescence. This is also evident from the decreasing plot of fluorescence intensity versus [*Q*] (concentration of quencher) (inset of Fig. 1). Under identical conditions, there was no fluorescence emission for PAH at the investigated concentration. Further, the quenching was accompanied with an evident red shift (from 340 to 352 nm), which signified that the binding of PAH was associated with changes in the microenvironment of HSA.

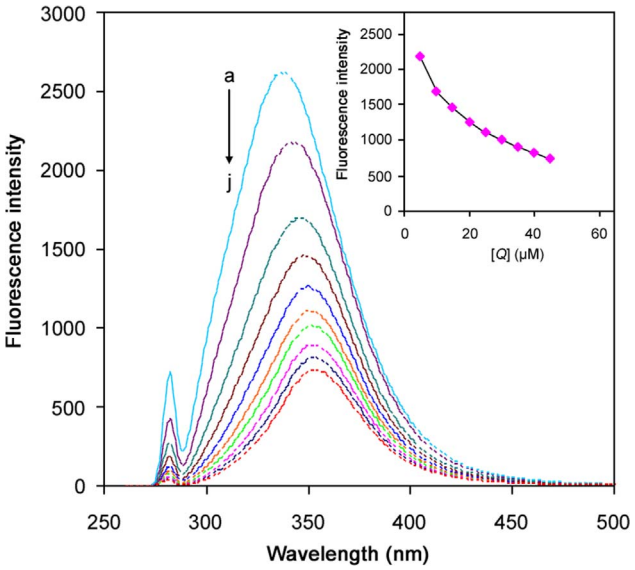

Fig. 1. Fluorescence quenching spectra of HSA at different concentrations of PAH at 298 K (λ_{ex}=280 nm). cHSA=5 μM; cPAH curves (a–j): 0, 5, 10, 15, 20, 25, 30, 35, 40 and 45 μM. Inset: Decreasing plot of fluorescence intensity at different concentrations of PAH.

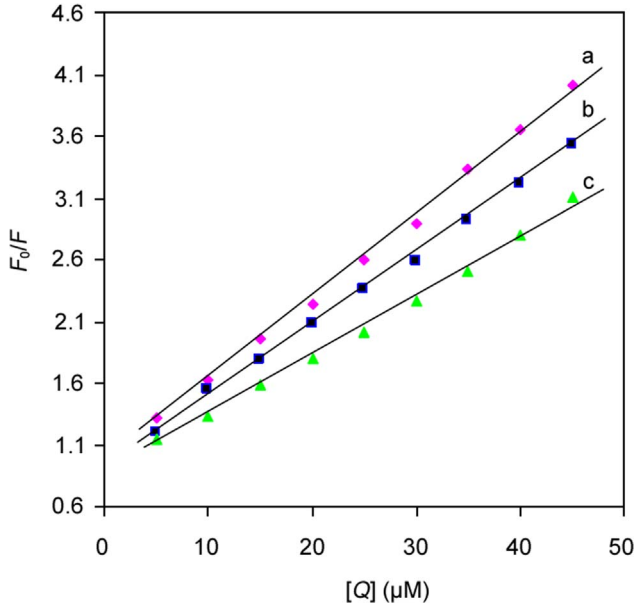

Fig. 2. Stern –Volmer plots for the binding of PAH with HSA at 288 K (a), 298 K (b) and 308 K (c).

3.2. Mechanism of binding mode

Fluorescence quenching is usually classified as dynamic and static quenching [21]. They can be distinguished by their difference on temperature dependence. The quenching rate constants decrease with increase in temperature for static quenching while reverse is true for dynamic quenching [23]. To analyze the quenching mechanism, the fluorescence intensity data obtained at different temperatures were subjected to Stern–Volmer quenching equation [24],

$$\frac{F_0}{F} = 1 + K_{SV}[Q] \tag{1}$$

where F_0 and F are the steady state fluorescence intensities of HSA before and after the addition of quencher (PAH), K_{SV} is the Stern–Volmer collisional quenching constant, and [Q] is the concentration of quencher (PAH), respectively.

Stern-Volmer plots of F_0/F versus [Q] at different temperatures are shown in Fig. 2. The plots exhibit a good linear relationship, which is generally indicative of the purely collisional or static quenching process [25]. The K_{SV} values were calculated from the slope of F_0/F versus [Q] (Fig. 2) at different temperatures. The values are given in Table 1. These values were found to decrease with increase in temperature, indicating that static type of quenching mechanism is operative. For a bimolecular quenching process, the quenching rate constant (k_q) can be evaluated by employing the following equation:

$$k_q = \frac{K_{SV}}{\tau_0} \tag{2}$$

where τ_0 is the average lifetime of biomolecules in the absence of quencher and the value of τ_0 for tryptophan fluorescence in HSA [26] is 10^{-8} s. Upper limit of k_q expected for a diffusion controlled bimolecular process [27] is 10^{10} M^{-1} s^{-1}. High magnitude of k_q observed here (10^{12} M^{-1} s^{-1}) indicated that the quenching mechanism was initiated by complex formation between PAH and HSA rather than by dynamic collision [28]. Therefore, the data was further analyzed employing the modified Stern-Volmer equation [29],

$$\frac{F_0}{F_0 - F} = \frac{1}{f_a K_{SV}[Q]} + \frac{1}{f_a} \tag{3}$$

where f_a is the fraction of initial fluorescence which is accessible to quencher. From intercept and slope of the plot of $F_0/(F_0–F)$ versus $1/[Q]$, the values of f_a and K_{SV} were obtained respectively. The value of f_a was found to be 0.82 for PAH–HSA, indicating that only 82% of the initial fluorescence of protein was accessible for quenching.

Table 1
Stern-Volmer quenching constants, apparent binding constants, binding sites and thermodynamic parameters for PAH-HSA system at different temperatures.

Temp (K)	K_{SV} (×10^{-4}) (L/mol)	K_a (×10^{-5}) (L/mol)	n	ΔG^0 (kJ/K)	ΔH^0 (kJ/mol)	ΔS^0 (J/mol/K)
288	6.75	0.86	1.03	−27.19		
298	5.70	1.76	1.11	−27.97	52.87	277.8
308	4.86	3.60	1.20	−32.75		

3.3. Analysis of binding constants and binding sites

Equilibrium between free and bound molecules is given by Eq. (4), providing that small molecules bind independently to a set of equivalent sites on a macromolecule [30]:

$$\log\left(\frac{F_0 - F}{F}\right) = \log K_a + n \log(Q) \tag{4}$$

where K_a is the binding constant or the apparent association constant for drug–protein interaction and n is the number of binding sites. Thus, the values of K_a and n at different temperatures (Table 1) can be determined from the slope and intercept of plot of log $(F_0–F)/F$ versus log [Q] (Fig. S2), respectively. Value of n is equal to 1, indicating that there is one independent class of binding site on HSA for PAH. Further, the values of K_a increased with increase in temperature, and the increase in K_a may be caused by a slight expansion of the binding site which might accommodate more PAH molecules. The expansion of the binding site may also provide a larger hydrophobic area for binding, thus leading to increase in the value of K_a[31].

3.4. Thermodynamic parameters and nature of binding forces

Thermodynamic parameters relying on temperatures were analyzed to characterize the acting forces between drug and HSA. Basically, four types of interactions play vital roles in drug-biomacromolecule binding, namely hydrogen bonds, van der Waals forces, electrostatic forces and hydrophobic forces [32]. The thermodynamic parameters, enthalpy change (ΔH^0), entropy change (ΔS^0) and free energy (ΔG^0) of a reaction, are important for confirming binding mode. The temperature dependence of the binding constant was studied and HSA did not undergo any structural degradation at the selected temperatures (288, 298 and 308 K). These thermodynamic parameters were calculated using the following equations:

$$\log K_a = -\frac{\Delta H^0}{2.303\,RT} + \frac{\Delta S^0}{2.303R} \tag{5}$$

$$\Delta G^0 = \Delta H^0 - T\Delta S^0 \tag{6}$$

where K_a and R are the binding constant and gas constant, respectively. The values of ΔH^0 and ΔS^0 were evaluated from the linear plot of log K_a versus $1/T$. The results obtained are summarized in Table 1. Negative values of ΔG^0 reveal that the binding process is spontaneous. The positive entropy change occurs because the water molecules that are arranged in an orderly fashion around the drug and protein acquire a more random configuration as a result of hydrophobic interactions. In the present case, positive ΔH^0 and ΔS^0 indicate major contributions of hydrophobic interactions in the binding process. Indeed, the unfavorable enthalpy loss is cancelled by the much larger entropic gain which probably originates from the extensive dehydration from PAH and HSA, to give a very stable complex.

Table 2
The comparison of binding constants of PAH-HSA before and after the addition of site probe at 298 K.

Systems	Binding constants (L/mol)
HSA+PAH	1.767×10^5
HSA+PAH+Warfarin	1.540×10^4
HSA+PAH+Ibuprofen	1.714×10^5
HSA+PAH+Digitoxin	1.752×10^5

3.5. Competitive binding of site probes

In order to determine the specificity of PAH binding sites on HSA, displacement experiments were performed using site-selective probes viz., warfarin (site I), ibuprofen (site II) as per Sudlow's classification of binding sites [21]. Sjoholm et al. [9] have pointed out the digitoxin binding in protein is independent of Sudlow's site I and II, and perch on what was nominated as site III. According to Eq. (4), the binding constants in the presence of site probes were calculated from fluorescence data. Table 2 shows the binding constant of PAH–HSA in presence of different site probes. From Table 2, it is evident that the drug competes with warfarin for Sudlow's site I in the protein. This resulted in decreased binding constant. However, PAH was not significantly displaced by ibuprofen and digitoxin. Hence, the site I located in subdomain II A is anticipated to be the main binding site for PAH in HSA.

3.6. Fluorescence resonance energy transfer (FRET) between PAH and HSA

FRET is an excellent technique to determine the distance of separation between the donor (fluorophore) and acceptor in vitro and in vivo [25]. The FRET efficiency mainly depends on three parameters: (i) the distance between donor and acceptor (which must be within the specified Fösters distance of 2–8 nm); (ii) appreciable overlap between the donor fluorescence and acceptor absorption band; and (iii) proper orientation of the transition dipole of the donor and acceptor.

According to Förster's theory [33], the energy transfer efficiency (E) is related not only to the distance (r) between acceptor and donor, but also to the critical energy transfer distance or Försters radius (R_0) and can be expressed as

$$E = 1 - \frac{F}{F_0} = \frac{R_0^6}{R_0^6 + r^6} \tag{7}$$

where E is the efficiency of energy transfer, F and F_0 are the fluorescence intensities of donor in the presence and absence of the acceptor, r represents the acceptor-donor distance, and R_0 is the critical distance when the transfer efficiency is 50%. R_0 can be expressed as below

$$R_0^6 = 8.8 \times 10^{-25} k^2 N^{-4} \phi J \tag{8}$$

where k^2 is the spatial orientation factor of the dipole (2/3), N is the refractive index of the medium (1.336), Φ is the fluorescence quantum yield of the donor (0.15), and J is the overlap integral of the fluorescence emission spectrum of the donor and the absorption spectrum of the acceptor. J is given by

$$J = \frac{\sum F(\lambda)\varepsilon(\lambda)\lambda^4 \Delta\lambda}{\sum F(\lambda)\Delta\lambda} \tag{9}$$

where $F(\lambda)$ is the fluorescence intensity of the fluorescent donor of wavelength λ, and $\varepsilon(\lambda)$ is the molar absorption coefficient of the acceptor at wavelength λ. We observed a good overlap between the emission spectrum of tryptophan with absorption spectrum of the drug (Fig. 3). From the above equations we can calculate that J=1.089×10^{-14} cm^3 L/mol, R_0=2.59 nm, E=0.17 and r =4.28 nm.

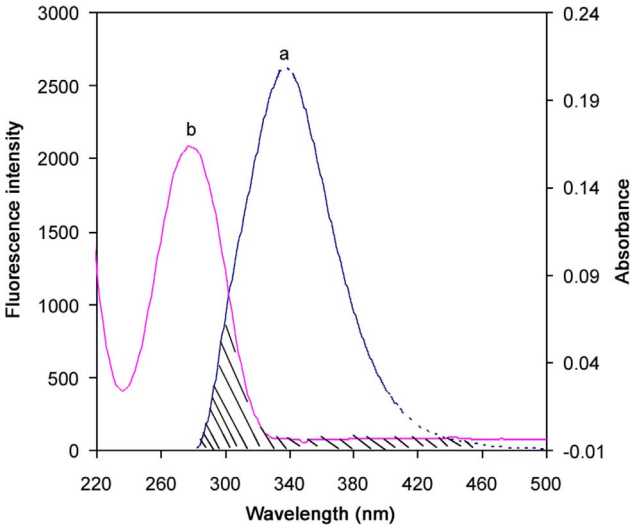

Fig. 3. Spectral overlap between fluorescence spectra of HSA (a) and absorption spectra of PAH (b). λ_{ex}=280 nm, λ_{em}=340 nm, cHSA=5 μM, cPAH=5 μM.

The value of r indicates that the donor and acceptor are close to each other and hence have strong binding between them. Further, as the observed donor-to-acceptor distance, r less than 8 nm revealed the presence of static type of quenching mechanism [34].

3.7. Influence of common ions on binding constant

Metal ions, especially those of bivalent type, are vital to human body and play an essentially structural role in many proteins based coordinate bonds [31]. The presence of metal ions in plasma may affect interaction of drugs with protein.

Therefore, effects of interference of some common ions on the binding constants of PAH–HSA system were investigated. It can be seen from the Table S1 that the presence of Zn^{2+} ion increases the binding constant of PAH–HSA system, whereas the presence of Ca^{2+}, Cu^{2+}, Mn^{2+}, Ni^{2+} and Co^{2+} decreases the binding constant of PAH–HSA system to various degrees. The higher binding constant possibly results from the formation of metal ion–PAH complexes via metal ion bridge [35]. This may prolong storage period of PAH in blood plasma and enhance its maximum effects. On the contrary, the decrease in the binding constant may be due to the formation of metal ion–protein complexes. The formation of such complexes is likely to affect conformation of protein, which may influence PAH binding kinetics and even inhibit PAH-HSA binding.

3.8. Conformational investigations

3.8.1. UV–vis absorption studies

UV–vis absorption measurement is a very simple method and applicable to explore structural changes and determine complex formation [27]. The λ_{max} value of HSA observed at around 280 nm was mainly due to the presence of tryptophan and tyrosine residues in HSA. It was evident from the spectrum for HSA (Fig. S3) that the absorption intensity of HSA increased regularly with increased concentration of PAH. Further, a slight red shift of the absorption maximum indicated the changes in polarity around tryptophan residues and changes in the peptide strand of the HSA molecule and hence in its hydrophobicity [36].

3.8.2. CD studies

CD is a sensitive technique to monitor the conformational changes in the protein. The CD spectra of HSA in the presence and absence of PAH are shown in Fig. 4. The CD spectrum of HSA exhibited two negative bands in the UV region at 208 and 220 nm, which are

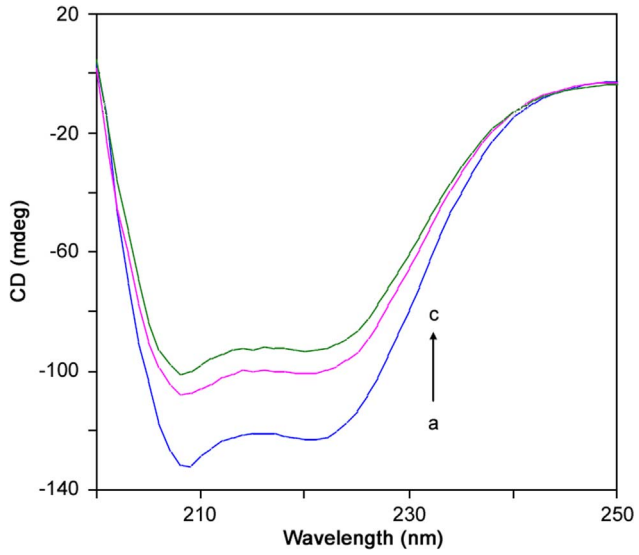

Fig. 4. CD spectra of HSA in the absence and presence of PAH from 200 to 250 nm. (a) cHSA=1 μM; (b) cHSA=1 μM, cPAH=1 μM; (c) cHSA=1 μM, cPAH=3 μM.

characteristic of an α–helical structure of protein [37]. The CD results are expressed in terms of mean residue ellipticity (MRE) in deg cm^2 $dmol^{-1}$.

$$MRE = \frac{Observed\ CD(mdeg)}{C_P nl \times 10} \quad (10)$$

where C_P is the molar concentration of the protein, n is the number of amino acid residues and l is the path length. The α–helical contents of free and combined HSA were calculated from MRE values at 208 nm using the following equation [37]

$$\alpha\text{–}helix(\%) = \frac{-MRE_{208} - 4000}{33000 - 4000} \times 100 \quad (11)$$

where MRE_{208} is the observed MRE value at 208 nm, 4000 is the MRE of the β–form and random coil conformation cross at 208 nm and 33,000 is the MRE value of a pure α–helix at 208 nm. Using the above equation, the α–helicity in secondary structure of HSA was calculated and was found to be decreased from 81.09% in free HSA to 62.43% in PAH–HSA complex. This was indicative of the loss of α–helicity upon interaction. Further, the CD spectra of HSA in the presence and absence of PAH did not show significant shift in the peaks, thereby indicating that the structure of HSA was predominantly α–helical even after binding [3].

3.8.3. Synchronous fluorescence

The SFS give information about the molecular environment in a vicinity of the chromosphere molecules and have several advantages, such as sensitivity, spectral simplification, spectral bandwidth reduction and avoiding different perturbing effects [36]. The amino acid residues environment was studied by measuring the possible shift in the emission maximum wavelength (λ_{max}). The shift of λ_{max} is related to the changes of the polarity around the chromophore molecule [38]. When D-value ($\Delta\lambda$) between excitation wavelength and emission wavelength is stabilized at 15 nm and 60 nm, the synchronous fluorescence gives characteristic information about the polarity of tyrosine (Tyr) and tryptophan (Trp) residue, respectively. The SFS are shown in Fig. 5. When $\Delta\lambda$ values were set at 15 and 60 nm, a red shift was observed in both with increasing concentration of PAH as seen in Fig. 5. The experimental results signify that the polarity around the Try and Trp residues increases and hydrophobicity decreases. This indicates the conformational changes in HSA in presence of PAH.

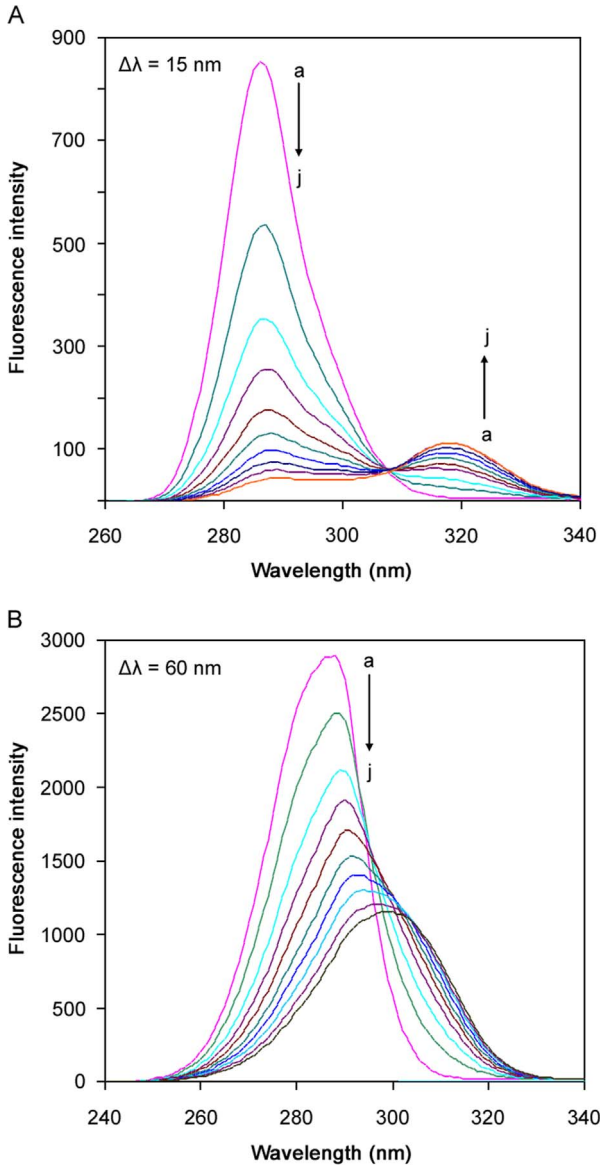

Fig. 5. Synchronous fluorescence spectra of HSA upon addition of PAH at 298 K when (A) $\Delta\lambda$=15 nm and (B) $\Delta\lambda$=60 nm. cHSA=5 μM; cPAH curves (a–j): 0, 5, 10, 15, 20, 25, 30, 35, 40 and 45 μM.

3.8.4. 3D fluorescence studies

3D fluorescence spectroscopy is a powerful and vigorous method for studying conformational and structural information of proteins. The 3D fluorescence spectra and the corresponding contour diagrams for HSA and HSA-PAH and the corresponding data are shown in Fig. 6 and Table 3. Peak a denotes the Rayleigh scattering peak (λ_{ex}=λ_{em}). Peak b mainly reflects the spectral characteristics of Trp and Try residues and peak c is the second ordered scattering peak (λ_{em}=2λ_{ex}).

In Fig. 6, the fluorescence intensity of peak a increased with the addition of PAH, and the possible reason might be due to the formation of complex formation between PAH–HSA. So the diameter of the macromolecule increased and resulted in the enhanced scattering effect [39]. Compared with the UV–vis absorption spectra of HSA (Fig. S3), there was an absorption peak around 280 nm and this peak was mainly caused by the transition of n→π* of proteins characteristic polypeptide backbone structure, C=O [40]. The fluorescence intensity of peak b decreased markedly and the maximum emission wavelength of the peak was changed following the addition of PAH. The analysis of the intensity changes of peak a and peak b revealed that the binding of

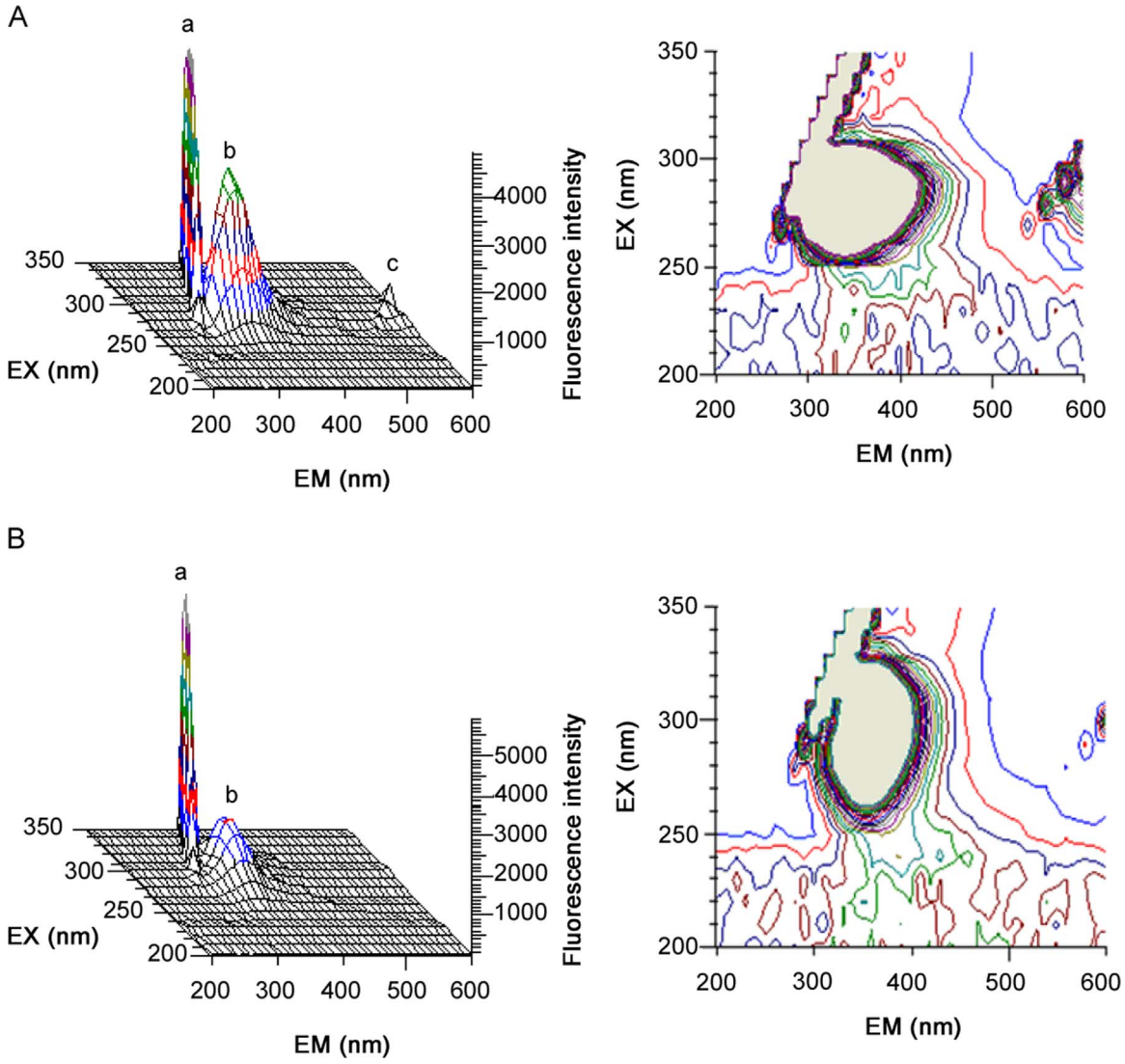

Fig. 6. Three-dimensional fluorescence spectra and corresponding contour diagrams of (A) HSA and (B) HSA-PAH. The concentration of HSA is fixed at 5 μM and that of PAH is fixed at 45 μM.

Table 3
Three-dimensional fluorescence spectral characteristic parameters of HSA and HSA–PAH system at 298 K.

System	Peaks	Peak position $\lambda_{ex}/\lambda_{em}$ (nm/nm)	$\Delta\lambda$ (nm)	Intensity
HSA	a	250/250–350/350	0	6.94–4406
	b	290/340	50	3026
HSA–PAH	a	250/250–350/350	0	8.19–5970
	b	290/340	50	1263

PAH to HSA induced some conformational and micro–environmental changes in HSA [41].

4. Conclusion

The interaction of PAH with HSA under simulated physiological condition was studied using different spectroscopic approaches. Experimental results showed that PAH is a strong quencher and interacts with HSA through static quenching mechanism. The values of thermodynamic parameters reveal that the binding is mainly entropy driven and hydrophobic interactions play a major role in stabilizing the complex. The distance between the donor (HSA) and the acceptor (PAH) was calculated using FRET. Conformational investigation results from UV–vis, CD, SFS and 3D fluorescence spectra revealed that the binding of PAH to HSA induced some micro-environmental and conformational changes. The results of this study provide important insights into the information of the structural features that determine the therapeutic effectiveness of PAH. Further, the study of drug-protein interactions guides to better understanding of pharmacokinetics such as drug metabolism, excretion and distribution.

Acknowledgments

Kirthi S. Byadagi gratefully acknowledges the UGC, New Delhi, India, for the award of Research Fellowship in science for Meritorious Students (RFSMS). The authors thank the Chairman, Department of Molecular Biophysics, Indian Institute of Science, Bangalore, India, for CD measurement facilities.

Appendix A. Supplementary material

Supplementary data associated with this article can be found in the online version at http://dx.doi.org/10.1016/j.jpha.2016.07.004.

References

[1] X.M. He, D.C. Carter, Atomic structure and chemistry of human serum albumin, Nature 358 (1992) 209–215.
[2] J. Chen, X.Y. Jiang, X.Q. Chen, et al., Effect of temperature on the metronidazole–BSA interaction: multi-spectroscopic method, J. Mol. Struct. 876 (2008) 121–126.
[3] Y.J. Hu, Y. Liu, X.S. Shen, et al., Studies on the interaction between 1-hexylcarbamoyl-5-fluorouracil and bovine serum albumin, J. Mol. Struct. 738 (2005) 143–147.
[4] Y.J. Hu, Y. Liu, J.B. Wang, et al., Study of the interaction between monoammonium glycyrrhizinate and bovine serum albumin, J. Pharm. Biomed. Anal. 36 (2004) 915–919.
[5] D.H. Ran, X. Wu, J.H. Zheng, et al., Study on the interaction between florasulam and bovine serum albumin, J. Fluor. 17 (2007) 721–726.
[6] D.C. Carter, J.X. Ho, Structure of serum albumin, Adv. Prot. Chem. 45 (1994) 153–203.
[7] T. Peters, All About Albumin. Biochemistry, Genetics and Medical Applications, Academic Press, San Diego, USA, 1996.
[8] K. Yamasaki, T. Maruyama, U. Kragh-Hansen, et al., Characterization of site I on human serum albumin: concept about the structure of a drug binding site, Biochim. Biophys. Acta 1295 (1996) 147–157.
[9] I. Sjoholm, B. Ekman, A. Kober, et al., Binding of drugs to human serum albumin: XI. The specificity of three binding sites as studied with albumin immobilized in microparticles, Mol. Pharmacol. 16 (1979) 767–777.
[10] F. Chiappori, P. D'Ursi, I. Merelli, et al., In silico saturation mutagenesis and docking screening for the analysis of protein–ligand interaction: the endothelial protein C receptor case study, BMC Bioinforma. 10 (2009) S3.
[11] W.H. Ang, E. Daldini, L. Juillerat-Jeanneret, et al., Strategy to tether organometallic ruthenium-arene anticancer compounds to recombinant human serum albumin, Inorg. Chem. 46 (2007) 9048–9050.
[12] F.M. Stearns, Determination of procainamide and N-acetylprocainamide by "high performance" liquid chromatography, Clin. Chem. 27 (1981) 2064–2067.
[13] J.S. Dutcher, J.M. Strong, S.V. Lucas, et al., Procainamide and N-acetylprocainamide kinetics investigated simultaneously with stable isotope methodology, Clin. Pharma. Ther. 22 (1977) 447–457.
[14] F.L. Cui, J. Fan, J.P. Li, et al., Interactions between1-benzoyl-4-p-chlorophenyl thiosemicarbazide and serum albumin: investigation by fluorescence spectroscopy, Bioorg. Med. Chem. 12 (2004) 151–157.
[15] J. Szpunara, A. Makarov, T. Pieper, et al., Investigation of metallodrug –protein interactions by size-exclusion chromatograpy coupled with inductively coupled plasma mass spectrometry (ICP-MS), Anal. Chim. Acta 387 (1999) 135–144.
[16] F. Lebrun, A. Bazus, P. Dhulster, et al., Influence of molecular interactions on ultra filtration of a bovine hemoglobin hydrolysate with an organic membrane, J. Memb. Sci. 146 (1998) 113–124.
[17] A.H.A. Clayton, M.A. Perugini, J. Weinstock, et al., Fluorescence and analytical ultracentrifugation analyses of the interaction of the tyrosine kinase inhibitor, tyrphostin AG1478-mesylate, with albumin, Anal. Biochem. 342 (2005) 292–299.
[18] Q.Q. Bian, J.Q. Liu, J.N. Tian, et al., Binding of genistein to human serum albumin demonstrated using trytophan fluorescence quenching, Int. J. Biol. Macromol. 34 (2004) 275–279.
[19] P.D. Ross, S. Subramanian, Thermodynamics of protein association reaction: forces contribution to stability, Biochemistry 20 (1981) 3096–3102.
[20] A. Sulkowska, Interaction of drugs with bovine and human serum albumin, J. Mol. Struct. 614 (2002) 227–232.
[21] G. Sudlow, D.J. Birkett, D.N. Wade, Further characterization of specific drug binding sites on human serum albumin, Mol. Pharmacol. 12 (1976) 1052–1061.
[22] A. Sulkowska, B. Bojko, J. Ro´wnicka, et al., Paracetamol and cytarabine binding competit–ion in high affinity binding sites of transporting protein, J. Mol. Struct. 792-793 (2006) 249–256.
[23] Y.J. Hu, Y. Liu, L.X. Zhang, Study of interaction between colchine and bovine serum albumin by fluorescence quenching method, J. Mol. Struct. 750 (2005) 174–178.
[24] F.L. Cui, J.L. Wang, Y.R. Cui, et al., Fluorescent investigation of the interactions between N-(*p*-chlorophenyl)-N'-(1-naphthyl)thiourea and serum albumin: synchronous fluorescence determination of serum albumin, Anal. Chim. Acta 571 (2006) 175–183.
[25] J.R. Lakowicz, Principles of Fluorescence Spectroscopy, 3rd ed, Springer, New York, 2006.
[26] C.X. Wang, F.F. Yan, Y.X. Zhang, et al., Spectroscopic investigation of the interaction between rifabutin and bovine serum albumin, J. Photochem. Photobio. A: Chem. 192 (2007) 23–28.
[27] L.D. Ward, Measurement of ligand binding to proteins by fluorescence spectroscopy, Methods Enzymol. 117 (1985) 400–414.
[28] W.R. Ware, Oxygen quenching of fluorescence in solution an experimental study of the diffusion process, J. Phys. Chem. 66 (1962) 455–458.
[29] S. Ashoka, J. Seetharamappa, P.B. Kandagal, et al., Investigation of the interaction between trazodone hydrochloride and bovine serum albumin, J. Lumin. 121 (2006) 179–186.
[30] M.R. Eftink, C.A. Ghiron, Fluorescence quenching studies with proteins, Anal. Biochem. 114 (1981) 199–227.
[31] X.Z. Feng, Z. Lin, L.J. Yang, et al., Investigation of the interaction between acridine orange and bovine serum albumin, Talanta 47 (1998) 1223–1229.
[32] P. Ju, H. Fan, T. Liu, et al., Probing the interaction of flower-like CdSe nanostructure particles targeted to bovine serum albumin using spectroscopic techniques, J. Lumin. 131 (2011) 1724–1730.
[33] T. Förster, Delocalized excitation and excitation transfer, O. Sinanoglu (Ed.), Modern Quantum Chemistry. Istanbul Lectures 3, Academic Press, New York/London, 1965, 93–137.
[34] F.L. Cui, J. Fan, D.L. Ma, et al., A study of the interaction between a new reagent and serum albumin by fluorescence spectroscopy, Anal. Lett. 36 (2003) 2151–2166.
[35] X.F. Liu, Y.M. Xia, Y. Fang, Effect of metal ions on the interaction between bovine serum albumin and berberine chloride extracted from a traditional Chinese herb *coptis chinensis franch*, J. Inorg. Biochem. 99 (2005) 1449–1457.
[36] W.Y. Qing, T.B. Ping, Z.H. Mei, et al., Studies on the interaction between imidacloprid and human serum albumin: spectroscopic approach, J. Photochem. Photobio. B: Biol. 94 (2009) 183–190.
[37] H. Gao, L. Lei, J. Liu, et al., The study on the interaction between human serum albumin and a new reagent with antitumour activity by spectrophotometric methods, J. Photochem. Photobio. A: Chem. 167 (2004) 213–221.
[38] N.L. Vekshin, Separation of the tyrosine and tryptophan components of fluorescence using synchronous scanning method, Biofizika 41 (1996) 1176–1179.
[39] F.F. Tian, F.L. Jiang, X.L. Han, et al., Synthesis of a novel hydrazone derivative and biophysical studies of its interactions with bovine serum albumin by spectroscopic, electrochemical and molecular docking methods, J. Phy. Chem. B 114 (2010) 14842–14853.
[40] A.N. Glazer, E.L. Smith, Studies on the ultraviolet difference spectra of proteins and polypeptides, J. Biol. Chemi. 236 (1961) 2942–2947.
[41] J. Juα´rez, S.G. López, A. Cambón, et al., Influence of electrostatic interactions on the fibrillation process of human serum albumin, J. Phy. Chem. B 113 (2009) 10521–10529.